Optics Communications 365 (2016) 76–85

Contents lists available at ScienceDirect

Optics Communications

journal homepage: www.elsevier.com/locate/optcom

# Eliminating zero spectra in Fourier transform profilometry by application of Hilbert transform

Feng Luo, Wenjing Chen*, Xianyu Su

*Opto-Electronic Department, College of Electronics and Information Engineering, Sichuan University, Chengdu, Sichuan 610064, China*

ARTICLE INFO

*Article history:*
Received 28 October 2015
Received in revised form
24 November 2015
Accepted 30 November 2015
Available online 10 December 2015

*Keywords:*
Three dimensional measurement
Fringe analysis
Fourier transform profilometry
Hilbert transform
Phase calculation

ABSTRACT

Hilbert transform has the features of inducing a phase shifting of 90 degree and removing the DC component. We propose a novel method based on the piecewise Hilbert transform to suppress the background intensity of the deformed fringe pattern using only one fringe pattern in Fourier transform profilometry according to the approximation that the background of the fringe is a slowly varying function and its distribution in each half period of the fringe can be regarded as a constant. In the method, Hilbert transform deals with each segmented fringe section to remove the DC component and then forms a result fringe whose background intensity is suppressed well by putting the fringe pieces together. The proposed method can enlarge the measurement range and reduce the measurement error of FTP. The theoretical analysis is given. Computer simulations and experimental results demonstrate the effectiveness of the proposed method.



## 1. Introduction

Optical 3D measurement techniques based on the structured light illumination are widely used in various kinds of research fields including biomedicine, industry inspection, dynamical process analysis and machine vision, etc because of the characteristics of non-contact, full field analysis and high speed. Among them, Fourier Transform Profilometry (FTP) can reconstruct the shape of the measured object from only one fringe or at most two fringes by Fourier transform, filtering in frequency domain and inverse Fourier transform. After proposed by M. Takeda and K. Muloh [1] in 1983, FTP is deeply studied and widely used [2–10]. Fourier transform provides excellent frequency resolution without spatial localization ability and the measurement range of Fourier transform profilometry is limited. If the zero frequency component and the high orders spectra component interfere the useful fundamental spectra, the reconstruction precision of FTP will decrease greatly. In order to overcome the disadvantage of Fourier transform, all kinds of methods have been proposed, such as the technology of quasi-sinusoidal projection and $\pi$ phase shifting for suppressing the zero frequency component and high orders spectra component [2], composite stripe projection technology for eliminating zero frequency component [4], color fringe projection technology for improving the accuracy and measurement range of FTP [5,6], wavelet transform method, empirical mode decomposition and Neural network, etc [7–15], to overcome the disadvantages of FTP. These techniques have their own applications according to the property of the measured objects. For example, $\pi$ shifting technique needs to capture two fringe patterns with $\pi$phase difference to eliminate the background intensity by subtracting operation, which improves the accuracy and measurement range but influences the real-time of FTP. It is a reliable method for measuring the static objects with high accuracy. In the method of projecting composite stripe, the background intensity can be eliminated from only one captured composite deformed fringe, but higher resolution of the CCD is needed to keep the separation between the useful component and the other components.

As we all know that the deformed fringe pattern is not periodic stationary anymore, because the projected sinusoidal fringe is modulated by the tested object. For analyzing the non-stationary fringe signal, Empirical mode decomposition combining with Hilbert transform is useful, in which Empirical mode decomposition decomposes the deformed fringe into Intrinsic Mode Functions (IMFs) varying from high frequency to low frequency. Then the separation of the zero frequency from the spectra would be operational [8–10], while Hilbert transform can be seen as 90 degree phase-shifter. If the background intensity of the fringe is eliminated by Empirical mode decomposition, a result analytic function can be obtained by Hilbert transform, from which the phase information can be calculated by the ratio of the imaginary part and the real part of the analytic function. The phase accuracy is high by this method, but the decomposition process is time-consuming.

* Corresponding author.
*E-mail address:* chenwj0409@scu.edu.cn (W. Chen).

http://dx.doi.org/10.1016/j.optcom.2015.11.073
0030-4018/

Because the background intensity and contract of the deformed fringe are slowly varying functions, the background distribution in each half period of the fringe can be regarded as a constant approximately [11,12]. Hilbert transform has the features of 90 degree phase shift and removing the DC component. Here a new method based on twice piecewise Hilbert transform is proposed to suppress background component of the fringe pattern. The method can suppress zero frequency component well and improve the measurement accuracy and range of FTP using only one fringe pattern. The theoretical analysis is given, and computer simulations and experiments are used to verify our analysis.

The organization of the paper is as follows: In Section 2, we give the principle of FTP and Hilbert transform. In Section 3, computer simulations are carried to compare the results obtained from the traditional FTP and FTP combining with Hilbert transform, respectively. While in Section 4, the experiments are applied to verify the effectiveness of proposed method. Last but not least, the conclusion is made in Section 5.

## 2. Principles

### 2.1. The principle of the Fourier transform profilometry

The scheme of the FTP measuring geometry is shown in Fig. 1 [1,7].

The optical axes of projector lens P1P2 crosses that of the camera lens I1I2 at point O on the reference plane which is perpendicular to the figure plane. L0 is the distance between point I2 and point O, d depicts the distance between P2 and I2. A and C are points on the reference plane. h is the height of the point D on the tested object $h(x, y)$. A sinusoidal grating image is projected onto the object surface. The deformed fringe pattern captured by CCD is expressed as:

$$f(x, y) = a(x, y) + b(x, y)\cos[2\pi f_0 x + \varphi_0(x, y) + \varphi(x, y)] \tag{1}$$

Where $a(x, y)$represents the background intensity, and $b(x, y)$ is the fringe contrast. $f_0$ denotes the carrier frequency. $\varphi_0(x, y)$ denotes the original phase caused by the non-telemetric light path of the measurement system, corresponding to the phase on the reference plane. $\varphi(x, y)$ denotes the modulation phase caused by the tested object.

The Fourier spectrum of Eq. (1) can be expressed as:

$$F(u, v) = A(u, v) + C(u - f_0, v) + C^*(u + f_0, v) \tag{2}$$

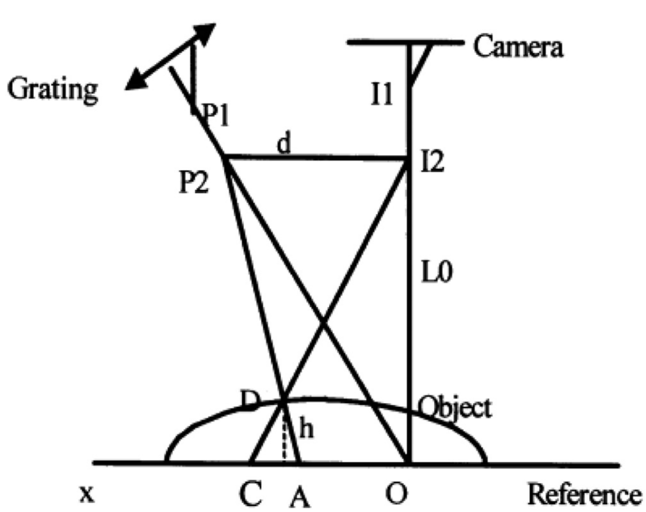


**Fig. 1.** Scheme of the FTP measuring geometry.

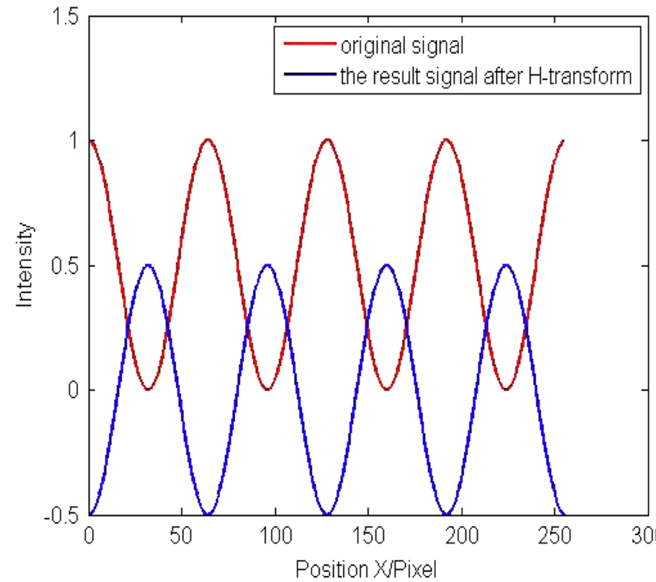


**Fig. 2.** Scheme of twice Hilbert transform.

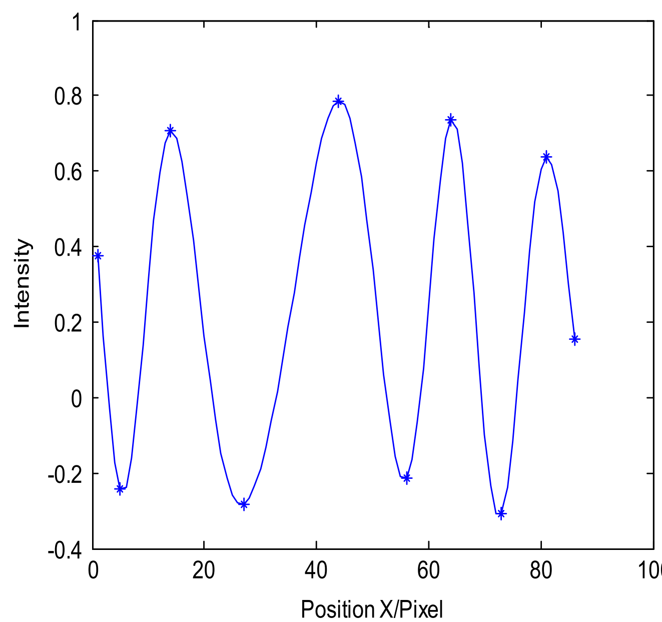


**Fig. 3.** A segment of a captured fringe pattern.

Where, superscript "*" expresses complex conjugate. $A(u, v)$ represents the zero spectra, corresponding the spectra of background component $a(x, y)$. $C(u - f_0, v)$ denotes the fundamental spectra contained the useful information of the measured object. $C^*(u + f_0, v)$ is the conjugate of $C(u - f_0, v)$. A suitable filter is used to select one of the fundamental spectra, such as $C(u - f_0, v)$. A complex exponential signal can be obtained by calculating the inverse Fourier transform of $C(u - f_0, v)$, which is expressed as:

$$g(x, y) = \frac{1}{2}b(x, y)\exp\{j[2\pi f_0 x + \varphi_0(x, y) + \varphi(x, y)]\} \tag{3}$$

From Eq. (3), the phase distribution $2\pi f_0 x + \varphi_0(x, y) + \varphi(x, y)$ can be obtained by extracted the complex angle of the complex signal. A reference fringe is dealt with to obtain the original phase $\psi_0(x, y)$ caused by the non-telemetric light path of the system. The phase map $\varphi(x, y)$ corresponding to the height distribution of the measured object can be obtained. Considering $L0 >> h(x, y)$ in the practical measurement, the relationship between the height

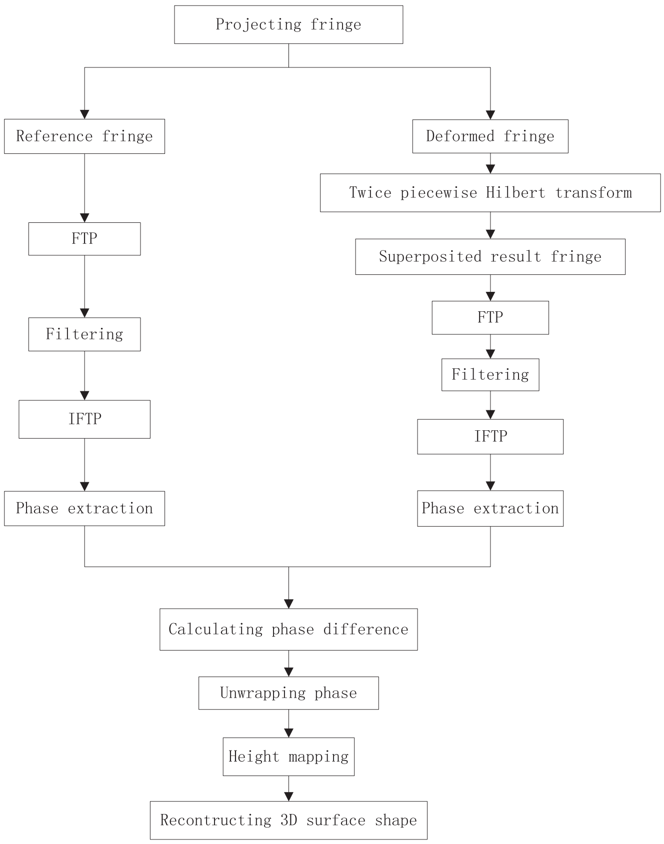


**Fig. 4.** Flowchart of principle of the proposed method.

variation of the object and the modulation phase $\varphi(x, y)$ can be approximately expressed as [1]:

$$\varphi(x, y) \approx \frac{2\pi f_0 d}{L0} h(x, y) \tag{4}$$

## 2.2. The principle of the Hilbert transform

The Hilbert transform of 1D signal $f(x)$ is defined as [15]:

$$H(f(x)) = \frac{1}{\pi}\int_{-\infty}^{+\infty} \frac{f(\tau)}{(x-\tau)} d\tau = \frac{1}{\pi x} * f(x) \tag{5}$$

Here superscript "*" expresses convolution operation. H means Hilbert transform. The Fourier spectra of $H(f(x))$ is expressed as:

$$\Im[H(f(x))] = -j\,\mathrm{sgn}(w)F(w) \tag{6}$$

Where $w$is the angular frequency, $\Im[\,]$ expresses the Fourier transform. $F(w)$ is the spectra of $f(x)$, $-j\,\mathrm{sgn}(w)$ is the spectra of $\frac{1}{\pi x}$. where $\mathrm{sgn}(w)$ is a sign function and is written as:

$$\mathrm{sgn}(w) = \begin{cases} -1, & w < 0 \\ 1, & w > 0 \end{cases} \tag{7}$$

Therefore, $-j\,\mathrm{sgn}(w)$ can be expresses as:

$$-j\,\mathrm{sgn}(w) = \begin{cases} e^{j\frac{\pi}{2}}, & w < 0 \\ e^{-j\frac{\pi}{2}}, & w > 0 \end{cases} \tag{8}$$

That means Hilbert transform can carry out 90 degree phase shifting for the positive frequency and $-90$ degree phase shifting for the negative frequency. In addition, by the Hilbert transform, the DC component is removed. If twice Hilbert transform is applied on the signal $f(x)$, its phase can shift 180 degree for either the positive or negative frequency. For example, the result of twice Hilbert transform of a sinusoidal fringe is shown in Fig. 2. The simulated signal is expressed as:

$$f(x) = 0.5 + 0.5\cos(2\pi x/p) \quad x = 0, 1, \ldots, 255 \tag{9}$$

where $p = 64(pixel)$ is the patch of the fringe. In the Fig. 2, the red line represents the original signal and the blue one represents the result signal after twice Hilbert transform. It shows that the constant background is eliminated and $\pi$ phase shift is introduced in the fringe.

When Hilbert transform is used to remove the zero frequency component of the deformed fringe pattern, the influence from nonuniform background intensity of the deformed fringe pattern is needed to be considered. It is impossible to remove the background of the fringe clearly by twice full field Hilbert transform. But the background and the contrast of the deformed fringe pattern change slowly, we can assume them to be uniform at local area. When Hilbert transform is carried out on the each segment of the fringe pattern, $a(x, y)$ and$b(x, y)$ can be regarded as a constant

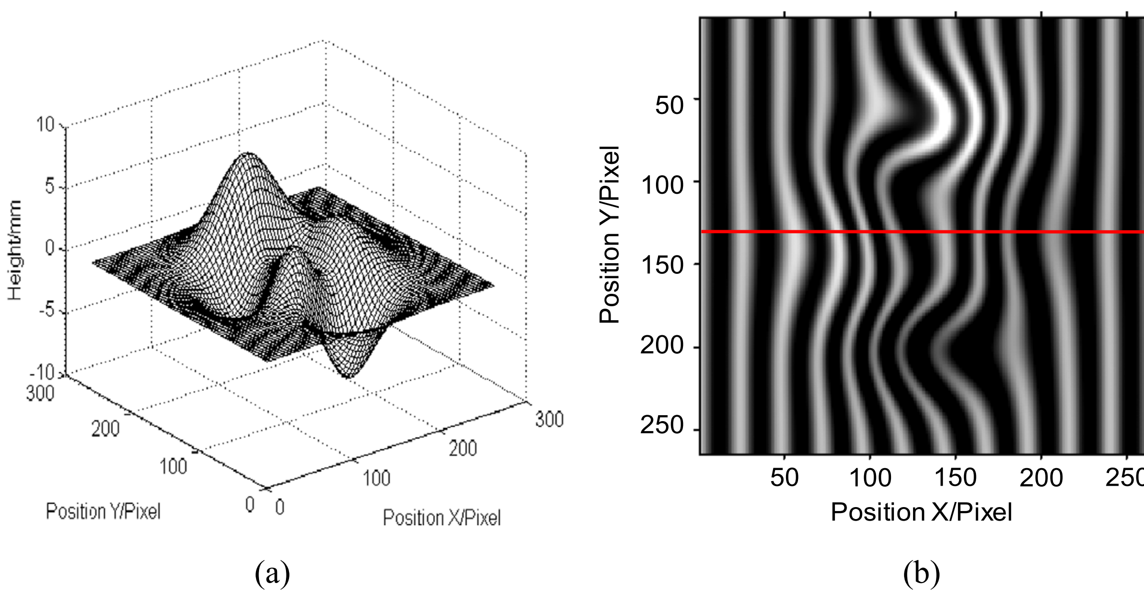


**Fig. 5.** (a) Simulated object;(b) deformed fringe pattern.

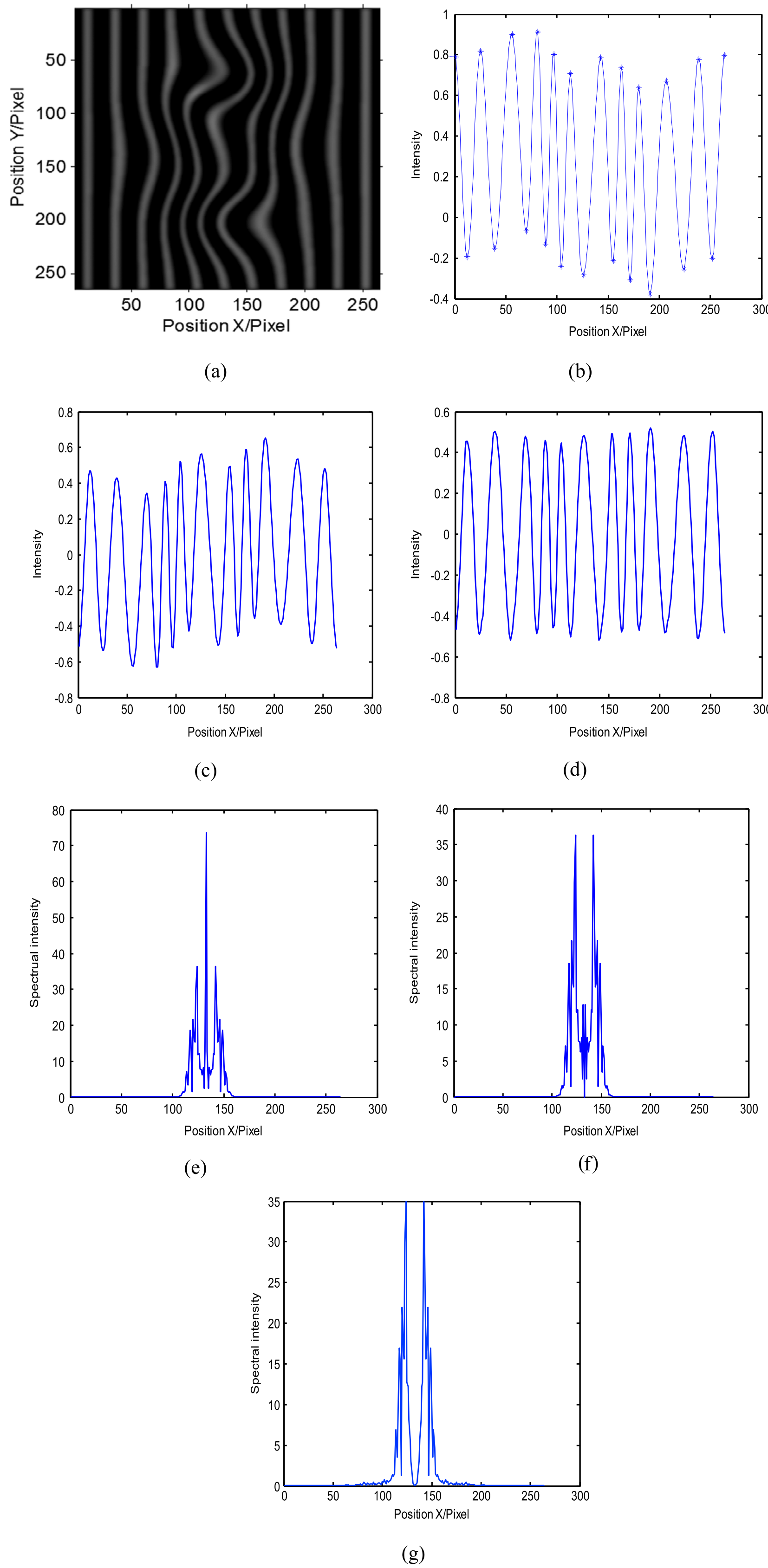


**Fig. 6.** (a) The result fringe by superposition of the fringe segments after twice Hilbert transform; (b) the 130th line of Fig. 5(b); (c) the 130th line of deformed fringe after twice full field Hilbert transform; (d) the 130th line of (a); (e) the spectra of (b); (f) the spectra of (c); (g) the spectra of (d).

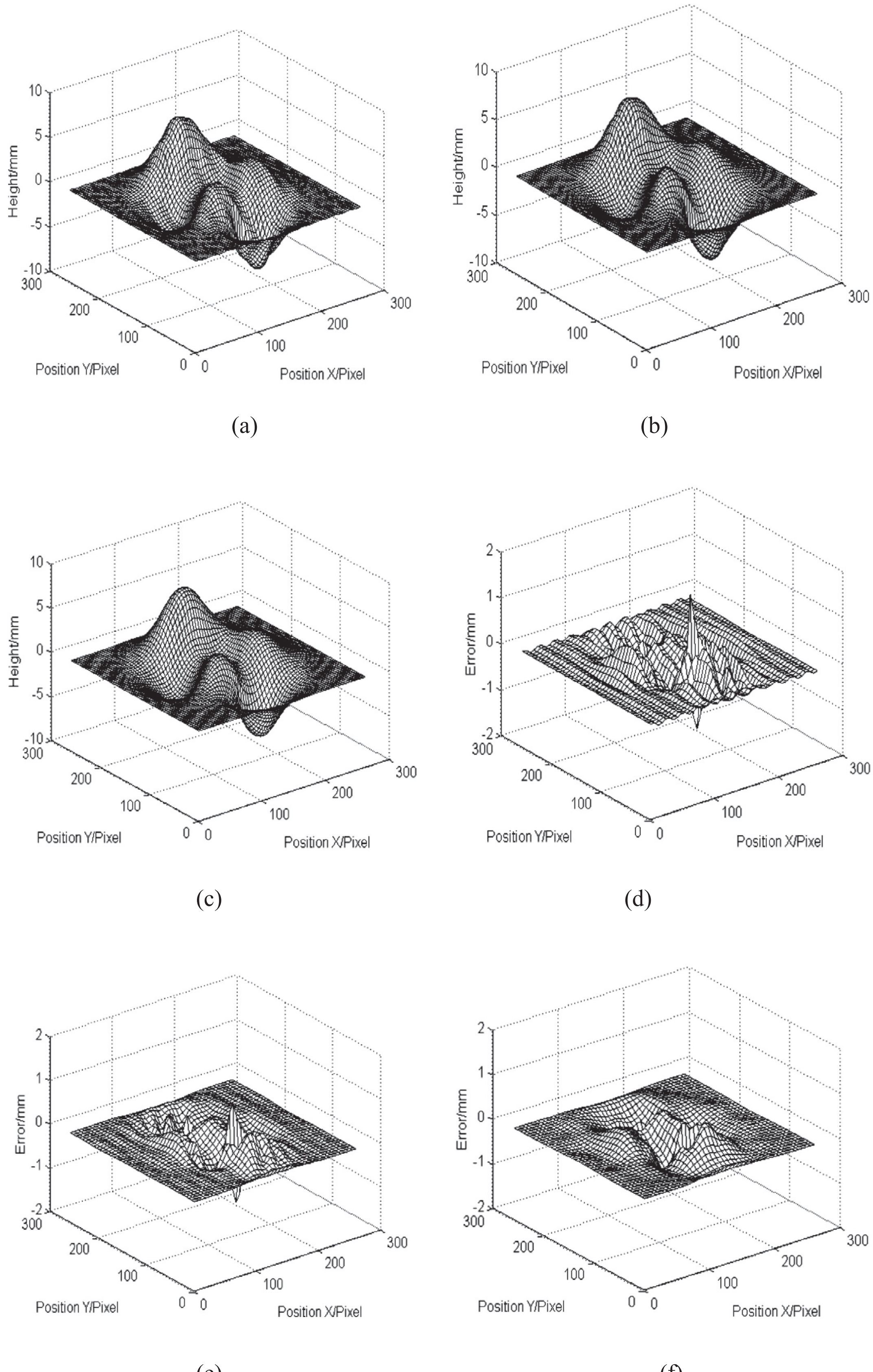


**Fig. 7.** (a) The reconstructed surface by FTP; (b) the reconstructed surface by FTP combining with twice full field Hilbert transform; (c) the reconstructed surface by FTP combining with twice piecewise Hilbert transform; (d) the error corresponding to (a); (e) the error corresponding to (b); (f) the error corresponding to (c).

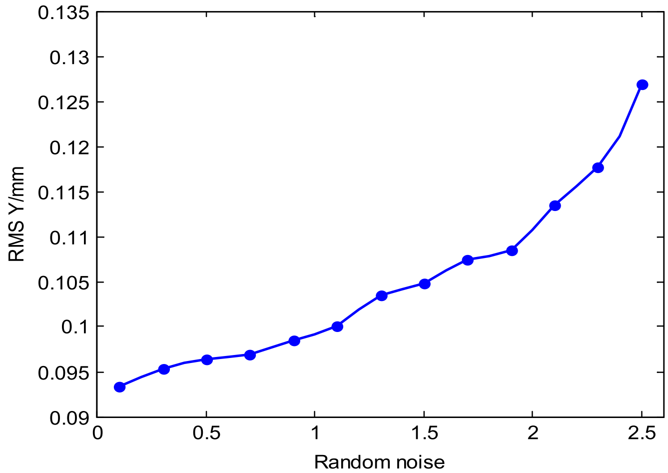


**Fig. 8.** The mean square errors under the different noise levels.

[11,12] in each segment with the length of half period of the each row of the fringe. Making 1D case as an example, without considering the variable y, any row of the $f(x, y)$ can be expressed as $f(x)$ and each segment of the line can be written as:

$$f_i(x) = a_i + b_i \cos\left[2\pi f_0 x + \varphi_0(x) + \varphi_i(x)\right] \quad i = 1, 2, \ldots, n \tag{10}$$

Where $f_i(x)$ indicates the $i$th segment of the line, $n$ represents the number of half period of the line, $a_i$ and $b_i$denote the background intensity and the fringe contrast respectively in the $i$th half period. $\psi_i(x)$ denotes the modulation phase resulting from the object in the segment. Because the deformed fringe pattern is non-stationary, the number of the sampling points in each segment is not equal. The length of the each segment equals to the distance of between adjacent local maximum and local minimum. As shown in Fig. 3, the extreme points are marked by "*" in the fringe pattern. In fact, the fringe $f(x)$ can be written in vector$[f_1(x), f_2(x), f_3(x), \ldots, f_n(x)]$.

As shown in Fig. 2, the background constant can be removed and the 180 degree phase shifting is achieved after twice Hilbert transform. For practical fringe with nonuniform background intensity, given each half period of the fringe has uniform intensity, the background of these fringe segments can be removed by twice Hilbert transform. The combination of these result local fringe segments without DC component after twice Hilbert transform forms the result fringe pattern, in which the background is suppressed well and the phase changes 180 degree. Then FTP method is used to deal with the fringe pattern, both the measurement accuracy and range can be improved because the influence from the zero frequency component is suppressed. The basic flow of the proposed method is shown in Fig. 4.

Where twice Hilbert transform of each fringe segment $f_i(x)$ can be achieved by the following Matlab codes. A complex analytic signal of real function can be obtained by "Hilbert" function provided by Matlab function set. The imaginary part of the complex analytic signal is the Hilbert transform of the fringe segment, which is exacted by function "imag".

```
D1=hilbert( fi(x));
D11=-imag(D1);
D2=hilbert(D11);
D22=-imag(D2).
```

The above codes are placed in a for-loop to deal with all fringe segments, and the result fringe can be obtained by superposition of the fringe segments after twice Hilbert transform.

## 3. Computer simulations

In order to verify the method, some computer simulations are carried out. The simulated object is expressed as: $shape = 0.95{*}peaks(x, y)$, as shown in Fig. 5(a). The $peaks(x, y)$ function provided by Matlab platform is expressed as:

$$\begin{aligned} peaks(x, y) = {} & 3 \times (1 - x)^2 \times \exp(-(x^2) - (y+1)^2) - \\ & 10 \times (x/5 - x^3 - y^5) \times \exp(-x^2 - y^2) \\ & - 1/3 \times \exp(-(x+1)^2 - y^2) \end{aligned} \tag{11}$$

The simulated reference fringe pattern $f(x, y)$ and the simulated deformed fringe pattern $fs(x, y)$ are described as follows:

$$f(x, y) = 0.5 + 0.5 \times \cos(2\pi f_0 x) \tag{12}$$

$$fs(x, y) = -0.4 \times \frac{peaks}{Max_{peaks}} + 0.3 + 0.5 \times \cos[2\pi f_0 x + shape] \tag{13}$$

Where $f_0 = \frac{1}{24}(1/pixels)$,$Max_{Peaks}$ is the maximum of $peaks$ function. The size of the fringe pattern and the simulated object is $264 \times 264 pixels$. Assuming $2\pi f_0 d/L0 = 1$ in the Eq. (4), the word "shape" represents phase modulation caused by height variation. In order to simulate the zero frequency component extension of the deformed fringe pattern, $-0.4 \times \frac{Peaks}{Max_{Peaks}}$ is added to the simulated deformed fringe pattern to represent the nonuniform background distribution of the fringe pattern. The simulated deformed fringe pattern is shown in Fig. 5(b), in which the 130th row is marked by a red line for the next analysis.

The result fringe after twice piecewise Hilbert transform is shown in Fig. 6(a). For clarity and comparison, Fig. 6(b), (c) and (d) denote intensity distribution of the 130th line of the deformed fringe pattern, the result deformed fringe pattern after twice full field Hilbert transform and the result deformed fringe pattern after twice piecewise Hilbert transform respectively. In the Fig. 6(b), "*" are extreme point positions of the line which are used to determine the segment lengths of each segment. Compared with Fig. 6(b), the phase of the fringe in Fig. 6(c) and (d) shows 180 degree phase shift. In Fig. 6(c), the background distribution of the fringe after twice full field Hilbert transform is not suppressed well, but background distribution of the fringe after twice piecewise Hilbert transform, shown in Fig. 6(d) almost tends to be eliminated. Fig. 6(e), (f) and (g) are the spectra of Fig. 6(b), (c) and (d) respectively. We can find that the spectra becomes zero at the point f=0 and the slowly varying background corresponding zero frequency component extension still exists in Fig. 6(f). However, Fig. 6(g) shows that zero frequency component and its extension corresponding to the nonuniform background distribution of the fringe after twice piecewise Hilbert transform are suppressed well.

Fig. 7(a)–(c) denote the reconstructed surface by traditional Fourier transform profilometry, FTP combining with twice full field Hilbert transform and FTP combining with twice piecewise Hilbert transform respectively. We can find that the reconstructed surface shown in Fig. 7(c) is the best among the three figures because the zero frequency component and its extension of the deformed fringe pattern after twice piecewise Hilbert transform are suppressed well. Fig. 7(d)–(f) are the error maps correspondingly. The maximum errors are 1.752 mm, 1.4324 mm and 0.6976 mm, respectively. Their mean square errors are 0.1049 mm, 0.0931 mm and 0.0859 mm, respectively.

The effect of random noise in the proposed method is discussed. k times random noise generated by the rand function provided by Matlab function set are added to the Fig. 5 (b) respectively, where $k$ changes from 0.1 to 2.5 with interval 0.2. The distribution of mean square errors under the different noise

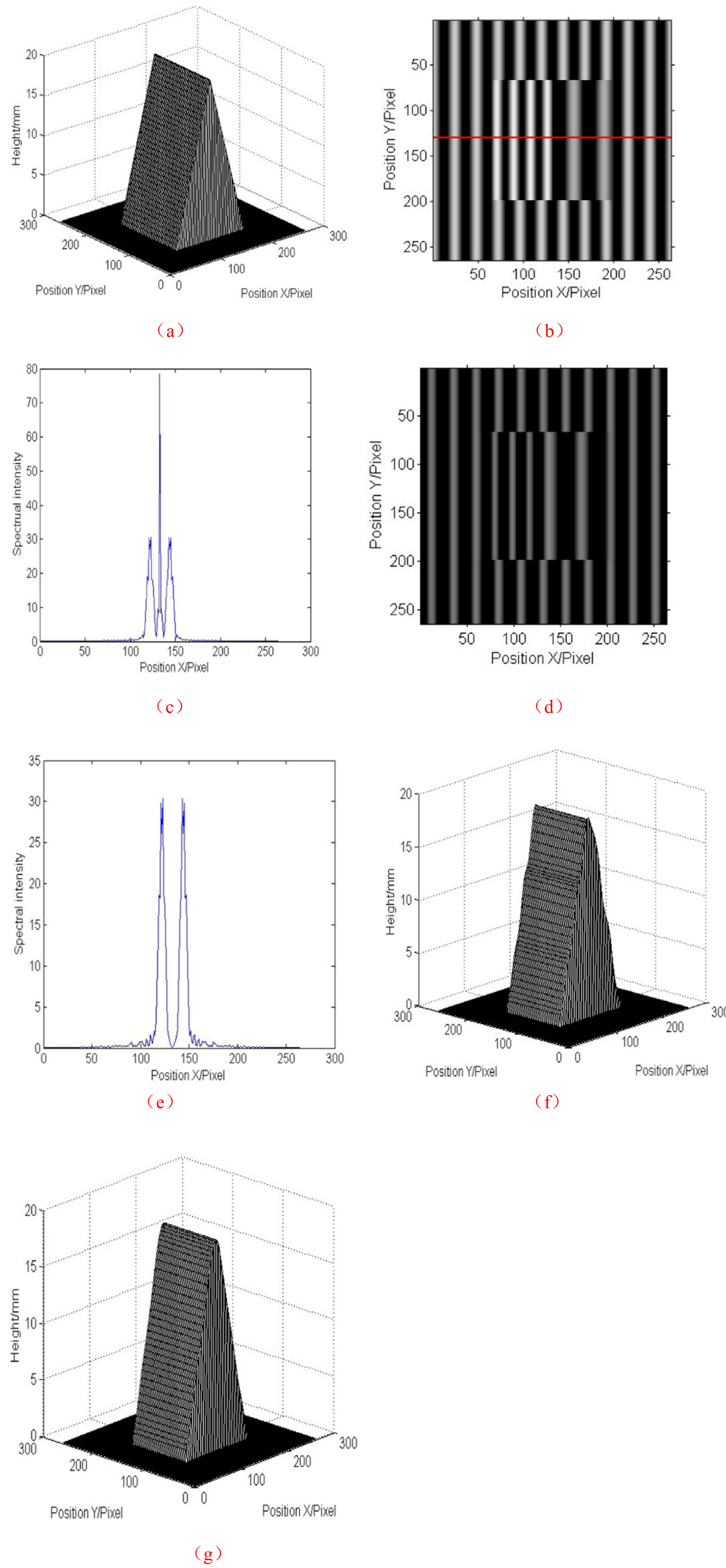


**Fig. 9.** (a) The simulated object; (b) the deformed fringe pattern; (c) the spectra of the 130th line of (b); (d) the result fringe by superposition of the fringe segments after twice Hilbert transform; (e) the spectra of the 130th line of (d); (f) the reconstructed surface from (b) by FTP; (g) the reconstructed surface from (d) by FTP combining with twice piecewise Hilbert transform.

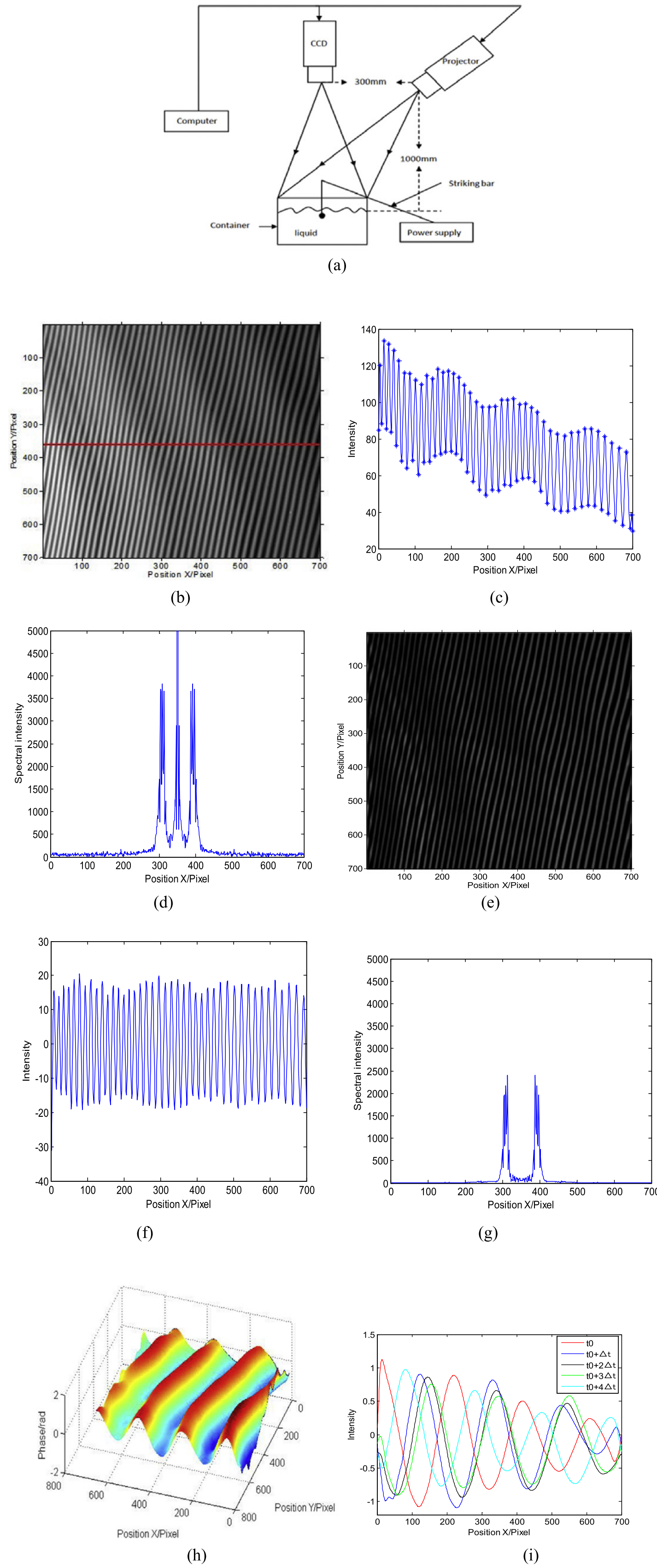


**Fig. 10.** (a) The schematic diagram of experimental setup; (b) one of the deformed fringes; (c) the 360th line of the deformed fringe after noise pretreatment; (d) the spectra of (c); (e) the result fringe after twice piecewise Hilbert transform; (f) the 360th line of (e); (g) the spectra of (f); (h) the reconstructed surface from (e); (i) the sections of wave ripples at different time.

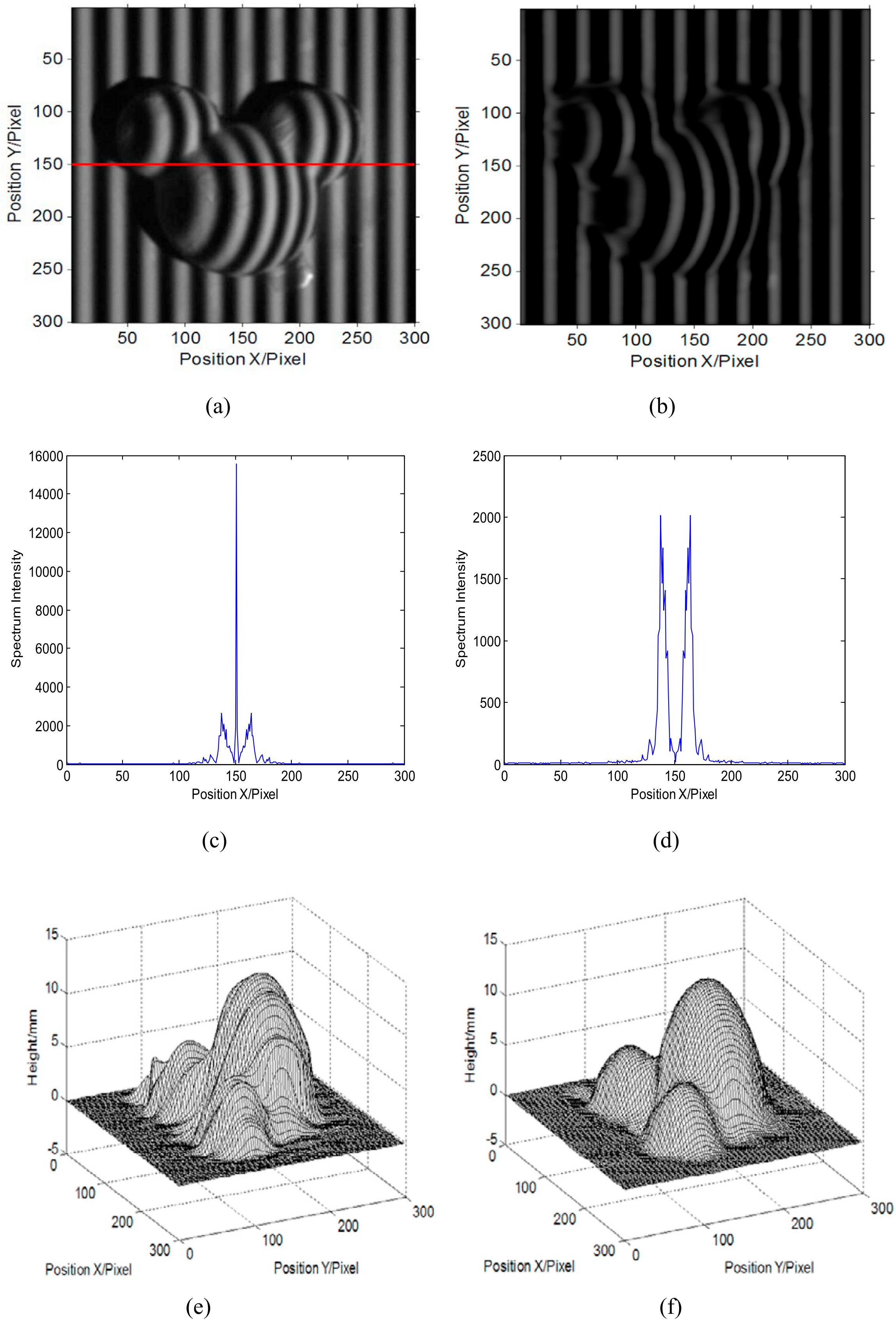


**Fig. 11.** (a) The deformed fringe pattern; (b) the result fringe pattern after twice piecewise Hilbert transform; (c) the Fourier transform spectra of the 150th line of the (a); (d) the Fourier transform spectra of the same line of the(b); (e) the reconstructed 3D shape of the 'Mickey' by the traditional FTP; (e) the reconstructed 3D shape of the 'Mickey' by the improved FTP.

levels is shown in Fig. 8. It shows that error will rise with the increase of noise.

A simulated triangle object is measured to verify how the algorithm performs in the case of the physical discontinuity in the measured object, because there are physical discontinuities on the ridge and the edges of the object, as shown in Fig. 9(a). The deformed fringe pattern is shown in Fig. 9(b) and Fig. 9(c) gives the spectra of the 130th line of the Fig. 9(b). Fig. 9(d) is the result fringe obtained by twice piecewise Hilbert transform and Fig. 9(e) is the spectra of the 130th line of the Fig. 9(d). The reconstructed surfaces from Fig. 9(b) and (d) are shown in Fig. 9(f) and (g), respectively.

## 4. Experiment

Removing the zero frequency component from only one deformed fringe pattern can improve the measurement accuracy and range and keep the real-time property of FTP. The improved FTP based on Hilbert transform is applied to measure the dynamic processing. The schematic diagram of experimental device is shown in Fig. 10(a). The projection equipment is DLP Lightcrafer 4500, and its mirror array size is 912*1140 pixels. The imaging CCD is Baumer (sxc100) with 1024*1024 pixels. The camera can synchronize with the projector employing the trigger signal given by the synchronization controlling units of the DLP Lightcrafer 4500. In the experiment, the sinusoidal structured light is projected onto a poster paint liquid, a set of deformed fringes formed by beating a basin of the liquid are captured for reconstructing the wave ripples. The size of the projected sinusoidal fringe is 912*1140 pixels with 10 pixels per period. 700*700 pixels area of one of the captured deformed images at a certain time is cut out for verifying the effect of eliminating the non-uniform background, as shown in Fig. 10(b). For clarity, the 360th line of the deformed fringe marked by the red line is shown in Fig. 10(c), in which the nonuniform background distribution is obvious.

In Fig. 10(c), the symbol "*" marks the extreme points. In the process of dealing with the practical deformed fringe pattern, a noising pretreatment (Gaussian smoothing filtering) is needed to eliminate false extreme points and make sure that the segment lengths of the fringe can be calculated correctly. The nonuniform background distribution will lead the zero frequency component to extend, as shown in Fig. 10(d), which will influence the measurement accuracy of the FTP. In order to eliminate the zero frequency component and its extension, twice piecewise Hilbert transforms are employed. The result fringe pattern is obtained by connecting the result fringe segments after twice piecewise Hilbert transform, as shown in Fig. 10(e). Fig. 10(f) and (g) show the intensity distribution of the 360th line of the result fringe pattern and its spectra. The zero frequency component and its extension are suppressed well in Fig. 10(g). The reconstructed surface from Fig. 10(e) is shown in Fig. 10(h). If all deformed fringes captured during a time period are processed, a dynamic 3D distribution of water wave ripple changing over time can be obtained. The 360th line sections of the reconstructed wave ripples at five different times are drawn in Fig. 10(i), in which $t0$ is the start time, $\Delta t$ is the time interval.

Another experiment is used to compare the measurement results of a mask 'Mickey' by the traditional FTP and the improved FTP based on twice piecewise Hilbert transform. The deformed fringe pattern with nonuniform background is shown in Fig. 11(a). The result fringe pattern after twice piecewise Hilbert transform is shown in Fig. 11(b). The Fourier transform spectra of the 150th line of the Fig. 11(a) is shown in Fig. 11(c), and the Fourier transform spectra of the same line in the Fig.11(b) is shown in Fig. 11(d), in which the zero frequency component and its extension are suppressed well. The reconstructed 3D shape of the 'Mickey' by the traditional FTP and improved FTP are shown in Fig. 11(e) and (f) using the same filter, respectively.

## 5. Conclusion

In this paper, twice piecewise Hilbert transform method is proposed to suppress zero frequency component from only one deformed fringe pattern, according to the approximation that the background of the fringe is a slowly varying function and its distribution in each half period of the fringe can be regarded as a constant. In the method, Hilbert transform deals with each segmented fringe section twice to remove the DC component. Then a result fringe whose background intensity is suppressed well is formed by putting these fringe pieces together. Finally the combined fringe pattern is conducted by the FTP method to reconstruct the shape of the object. Computer simulations and experimental results demonstrate the effectiveness of the proposed method in the application of eliminating the nonuniform background of the fringe.

## Acknowledgment

The authors acknowledge the support by National Key Scientific Apparatus Development project (2013YQ49087901) and Sichuan Talent Fund ([2015] 100-12).

## References

[1] M. Takeda, K. Mutoh, Fourier transform profilometry for the automatic measurement of 3-D object shapes[J], Appl. Opt. 22 (24) (1983) 3977–3982.
[2] Su Xian-yu, Chen Wen-jing, Fourier transform profilometry: a review[J], Opt. Lasers Eng. 35 (5) (2001) 263–284.
[3] Xian-Yu Su, Wen-Jing Chen, Qi-Chan Zhang, Yi-Ping Chao, Dynamic 3-D shape measurement method based on FTP, Opt. Lasers Eng. 36 (1) (2001) 49–64.
[4] C. Guan, L.G. Hassebrook, D.L. Lau, Composite structured light pattern for three dimensional video, Opt. Express 11 (5) (2003) 406–407.
[5] Da Fei-peng, Huang Hao, A novel color fringe projection based Fourier transform 3D shape measurement method[J], Optik 123 (24) (2012) 2233–2237.
[6] Wenjing Chen, Peng Bu, Suzhen Zheng, Xianyu Su, Study on Fourier transforms profilometry based on bi-color projecting, Opt. Laser Technol. 39 (2007) 821–827.
[7] M.A. Gdeisat, D.R. Burton, M.J. Lalor, Eliminating the zero spectrum in Fourier transform profilometry using a two-dimensional continuous wavelet transform, Opt. Commun. 266 (2006) 482–489 , October.
[8] N.E. Huang, Z. Shen, S.R. Long, The empirical mode decomposition and the Hilbert spectrum for nonlinear and non-stationary time series analysis, J. Proc. Lond. A G. B. 454 (1998) 903–995.
[9] X. Zhou, H. Zhao, T. Jiang, Adaptive analysis of optical fringe patterns using ensemble empirical mode decomposition algorithm, Opt. Lett. 34 (2009) 2033–2035 , July.
[10] Z. Sarac, Evaluation of thermal lens fringes using Hilbert and Fourier transform methods, IET Sci. Meas. Technol. 5 (3) (2011) 81–87.
[11] Y. Tangy, W. Chen, X. Su, et al., Neural network applied to reconstruction of complex objects based on fringe projection[J], Opt. Commun. 278 (2) (2007) 274–278.
[12] J. Zhong, J. Weng, Phase retrieval of optical fringe patterns from the ridge of a wavelet transform[J], Opt. Lett. A Publ. Opt. Soc. Am. 30 (19) (2005) 2560–2562.
[13] S. Li, X. Su, W. Chen, Hilbert assisted wavelet transform method of optical fringe pattern phase reconstruction for optical profilometry and interferometry, Optik: Int. J. Light. Electron Opt. 123 (2012) 6–10.
[14] Chenxing Wang, Feipeng Da, Phase demodulation using adaptive windowed Fourier transform based on Hilbert-Huang, Opt. Express 20 (16) (2012) 18460.
[15] L. Jie, W. Ming, H.H.Z. Bin, Fringe analysis with Hilbert transform and its application to the measurement of aspheric mirror[C], Proc. SPIE 6723 (2007) 67231D-1.